

Pulsed laser operating on the first vibrational overtone of the CO molecule in the 2.5–4.2- μm range:

3. The gain and kinetic processes on high vibrational levels

N.G. Basov, A.A. Ionin, Yu.M. Klimachev, A.A. Kotkov, A.K. Kurnosov, J.E. McCord, A.P. Napartovich, L.V. Seleznev, D.V. Sinitsyn, G.D. Hager, S.L. Shnyrev

Abstract. The gain dynamics in the active medium of an overtone CO laser operating on the transitions between high vibrational levels is studied experimentally and theoretically. The gain dynamics is measured on the vibration–rotation transitions of the CO molecule [the $P(12)$ spectral line in the vibrational bands from $20 \rightarrow 18$ to $36 \rightarrow 34$] in CO–He and CO–N₂ laser mixtures. The maximum small-signal gain was 0.43 m^{-1} . The theoretical model of the CO laser was significantly improved. It was shown that multiquantum and asymmetric VV-exchange processes should be included in the analysis of the population dynamics of high vibrational levels of the CO molecule.

Keywords: CO laser, overtone vibrations, gain, VV exchange.

1. Introduction

Our work is a continuation of papers [1, 2] devoted to the experimental and theoretical study of the characteristics of a pulsed electroionisation overtone CO laser. It was experimentally demonstrated in these papers that the efficiency of pump energy conversion to the overtone laser radiation amounts to 11% in the multifrequency regime [1] and to 0.6% in the frequency-selective regime [2]. The overtone lasing was obtained on more than 400 lines in a broad (from 2.5 to 4.2 μm) wavelength range in overtone vibrational bands from $6 \rightarrow 4$ to $38 \rightarrow 36$. Many of these lines can be used in laser spectroscopy and for the transport of laser radiation through the atmosphere [3–5]. The features of formation of the emission spectrum of an overtone CO laser, which were observed for the first time, were also discussed in papers [1, 2]. The authors of these papers pointed out that a comparison of experimental and com-

putational data revealed the necessity of improving the kinetic model of the active medium of the CO laser with inclusion of multiquantum vibrational VV-exchange processes involving high vibrational levels [2].

In this paper, we present the experimental and theoretical study of the small-signal gain (SSG) dynamics. The aim of this study was to consider processes that affect the formation of the emission spectrum of the overtone CO laser operating on high vibrational transitions. We modified substantially the kinetic model of the active medium of the CO laser taking into account new data on stimulated-emission cross sections and the rate constants for multiquantum VV exchange between CO molecules. The model also includes the asymmetric VV exchange between carbon monoxide molecules [$\text{CO}(V+2) + \text{CO}(0) \rightarrow \text{CO}(V) + \text{CO}(1)$] and between CO and N₂ [$\text{CO}(V+2) + \text{N}_2(0) \rightarrow \text{CO}(V) + \text{N}_2(1)$] molecules.

2. Experimental

Experiments were performed on a cryogenic laser setup with a 1.2-m long active medium described in detail in papers [1, 2]. The optical cavity $\sim 3 \text{ m}$ in length consisted of a spherical (with a radius of curvature of 20 m) copper mirror mounted on the laser chamber and a diffraction grating (200 lines mm^{-1} , $\lambda_{\text{max}} = 3.2 \mu\text{m}$) operating in the autocollimation regime. The laser radiation was extracted from the cavity in the zero order of the diffraction grating; the laser-beam aperture was determined by an intracavity diaphragm 20 mm in diameter.

In the experiments, the overtone CO-laser oscillation started after the termination of a 25–30- μs current pulse. The time delay of the laser pulse relative to the pump pulse (from $\sim 70 \mu\text{s}$ to several hundred microseconds) was determined by the time interval required for the SSG in the active medium to achieve the threshold value in the laser cavity. This threshold value was changed by varying the intracavity optical losses. The optical losses were controlled by introducing into the cavity a plane–parallel CaF₂ plate mounted at a specific angle to the cavity axis. By varying this angle, we changed the optical losses arising from the radiation reflection from the plate. In some cases, several such plates were mounted inside the cavity.

The optical losses introduced by the remaining optical elements of the laser cavity (a highly reflecting mirror, a diffraction grating, the output mirror of the laser chamber) were measured separately for each element. The highest losses were introduced by the diffraction grating, for which

N.G. Basov, A.A. Ionin, Yu.M. Klimachev, A.A. Kotkov, L.V. Seleznev, D.V. Sinitsyn P.N. Lebedev Physics Institute, Russian Academy of Sciences, Leninskii prospekt 53, 119991 Moscow, Russia; tel./fax: (095)132 04 25, e-mail: aion@mail1.lebedev.ru

A.K. Kurnosov, A.P. Napartovich, S.L. Shnyrev State Scientific Centre of the Russian Federation ‘Troitsk Institute for Innovation and Thermo-nuclear Research’, 142190 Troitsk, Moscow oblast, Russia; tel. (095)334 04 50, e-mail: apn@triniti.ru

J.E. McCord, G.D. Hager Air Force Research Laboratory (AFRL), Albuquerque, New Mexico, USA

Received 6 November 2001

Kvantovaya Elektronika 32 (5) 404–410 (2002)

Translated by E.N. Ragozin

the loss factor arising from radiation scattering and absorption was equal to $9 \pm 1\%$, while the spectral coefficient of radiation extraction in the zero diffraction order rose almost from zero to 8% as the laser wavelength increased from 3.2 to 4 μm (see Ref. [2], Fig. 3c). The optical losses arising from the scattering and absorption of radiation inside and outside the discharge chamber (including diffraction losses) were negligible compared to the total losses in the cavity.

We calculated the threshold gain in the laser cavity using the optical loss measurements. Note that, apart from the above-listed losses determined experimentally, there occur losses in the active medium which exist for only a short period, when gas-dynamic waves initiated by the discharge propagate through the medium. The instant of their appearance and their duration are determined by acoustic processes. Under our experimental conditions, these processes lasted for $\sim 10^{-4}$ s. Such perturbations of the active medium may lead to errors in the determination of the instant of attainment of the SSG threshold.

The time characteristics of output laser pulses were measured with a cryogenic Au–Ge photodetector and recorded with a storage oscilloscope. The instant of onset of the pump pulse (the energy input) was taken as the origin of the time axis. The delay of the laser pulse was far greater than duration of its leading edge, which was of about several microseconds under our experimental conditions. The interrelation between the delay of the laser pulse and the intracavity optical losses was employed to investigate the dynamics of SSG build-up in the active medium of the overtone CO laser.

To describe the SSG build-up dynamics corresponding to different experimental conditions, two parameters were considered in the processing of experimental data. One of them is the time delay τ_d required for the SSG in the active laser medium to achieve a given value equal to 0.05 m^{-1} (when the minimal measured value of the SSG exceeded this value, we used a linear data extrapolation). Another parameter is the rise time τ_{max} during which the SSG increased from 20% to 80% of its maximum value α_{max} .

3. Experimental results

3.1 Small-signal gain

The build-up dynamics of SSG α was measured on five vibration–rotation transitions of the CO molecule for two laser mixtures: CO : He = 1 : 4 (a specific energy input of $320 \text{ J L}^{-1} \text{ Amagat}^{-1}$) and CO : N₂ = 1 : 9 ($380 \text{ J L}^{-1} \text{ Amagat}^{-1}$). The overtone CO laser was tuned to the $P(12)$ spectral line in the vibrational bands $20 \rightarrow 18$ ($\lambda = 3.041 \mu\text{m}$), $26 \rightarrow 24$ ($3.341 \mu\text{m}$), $29 \rightarrow 27$ ($3.512 \mu\text{m}$), $33 \rightarrow 31$ ($3.767 \mu\text{m}$), and $36 \rightarrow 34$ ($3.982 \mu\text{m}$). Fig. 1 shows the experimental data obtained in these measurements. As the number V ($V+2 \rightarrow V$) of vibrational transition increased, the time delay τ_d for these two laser mixtures increased similarly (Fig. 2a), varying from $\sim 70 \mu\text{s}$ ($V = 18$) to $\sim 170 \mu\text{s}$ ($V = 34$). In all these experiments, the rise time τ_{max} was approximately the same and equal to $100 \pm 30 \mu\text{s}$ on the average.

Therefore, these experimental data demonstrate a weak effect of the composition of the laser medium on the time dynamics of SSG growth. The temporal parameters of the gain increase measured experimentally are in good agreement with the measurements of the SSG dynamics in the

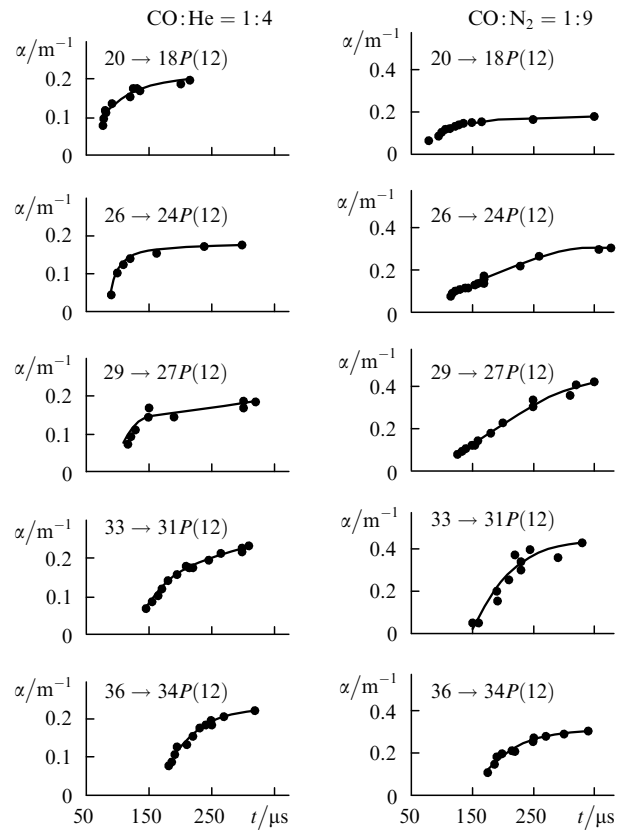


Figure 1. SSG dynamics measured for the $P(12)$ transition in the $20 \rightarrow 18$, $26 \rightarrow 24$, $29 \rightarrow 27$, $33 \rightarrow 31$, and $36 \rightarrow 34$ vibrational bands for the CO : He = 1 : 4 (specific energy input of $320 \text{ J L}^{-1} \text{ Amagat}^{-1}$) and CO : N₂ = 1 : 9 ($380 \text{ J L}^{-1} \text{ Amagat}^{-1}$) laser mixtures at a mixture density of 0.18 Amagat .

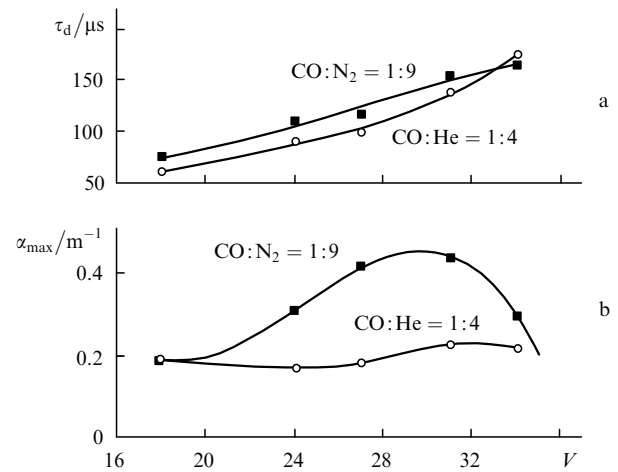


Figure 2. Time delay τ_d (a) and maximum SSG α_{max} (b) as functions of the vibrational level number V (the $V+2$ transition) for the data given in Fig. 1.

active medium of the overtone electroionisation CO laser performed using a master oscillator – amplifier laser system [6, 7].

Fig. 2b shows the dependence of the maximum SSG value α_{max} on the number of vibrational transition for two laser mixtures. In the nitrogen-free CO–He laser mixture, the α_{max} value was almost independent of the transition

number and was equal to $0.20 \pm 0.05 \text{ m}^{-1}$ for the vibrational transitions from $20 \rightarrow 18$ to $36 \rightarrow 34$, and also (see Section 3.2) for the $38 \rightarrow 36$ transition. In the helium-free CO–N₂ laser mixture, the dependence of α_{max} on the transition number V was different. As the transition number was increased, the α_{max} value initially increased from 0.18 m^{-1} (for the $20 \rightarrow 18$ transition) to 0.43 m^{-1} ($33 \rightarrow 31$), and then dropped sharply with increasing transition number.

3.2 Features of overtone lasing on high vibrational transitions

In Ref. [8], the absence of overtone lasing on the vibrational transitions higher than $37 \rightarrow 35$ was attributed to the conversion of vibrational energy corresponding to high vibrational levels of the electronic ground state of the CO molecule to the excitation energy of electronic states. In Ref. [2], the overtone lasing was nevertheless obtained on the spectral lines in the $38 \rightarrow 36$ band. In this case, the output characteristics of the overtone CO laser operating on the highest vibrational transitions were found to substantially depend on the nitrogen content in the laser gas mixture. In particular, when nitrogen was added to the CO–He laser mixture, the output pulse energy of the overtone CO laser operating on the $38 \rightarrow 36$ band lowered and that of the laser operating on the $36 \rightarrow 34$ band increased.

In this paper, we investigated the effect of nitrogen additions to the laser mixture on α_{max} and the output characteristics of the CO laser operating on the $38 \rightarrow 36$ vibrational band. Fig. 3 shows the dependence of α_{max} for the $38 \rightarrow 36$ $P(12)$ vibration–rotation transition on the nitrogen fraction X in the CO : He : N₂ = 1 : 4 : X laser gas mixture. In the nitrogen-free CO : He = 1 : 4 ($X = 0$) laser mixture, α_{max} was equal to $\sim 0.16 \text{ m}^{-1}$. When the concentration of nitrogen in the laser mixture was increased to $X = 0.3$, α_{max} reduced by about a factor of 1.5, down to the threshold value of the gain in the cavity with minimal optical losses (the horizontal dashed straight line in Fig. 3).

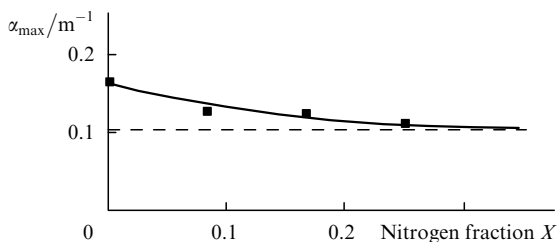


Figure 3. Maximum SSG value α_{max} for the $38 \rightarrow 36$ $P(12)$ transition as a function of the nitrogen fraction X in the CO : He : N₂ = 1 : 4 : X laser mixture at a mixture pressure of 0.12 Amagat and an energy input of $\sim 300 \text{ J L}^{-1} \text{ Amagat}^{-1}$.

A reduction of the SSG resulted in the variation of output laser characteristics. Fig. 4 displays the specific laser energy extraction (curve 1) and the threshold value of specific energy input (curve 2) as functions of nitrogen fraction in the laser mixture for minimal optical losses in the laser cavity. Small additions of nitrogen resulted in a decrease of laser energy extraction from $70 \text{ mJ L}^{-1} \text{ Amagat}^{-1}$ for $X = 0$ to nearly zero for $X = 0.25$ (a specific energy input of $\sim 300 \text{ J L}^{-1} \text{ Amagat}^{-1}$). Increasing the nitrogen fraction from zero to 0.42 caused the threshold value of specific

energy input to rise by more than a factor of two: from 170 to $370 \text{ J L}^{-1} \text{ Amagat}^{-1}$. For a specific energy input of $\sim 370 \text{ J L}^{-1} \text{ Amagat}^{-1}$, the duration of output laser pulse shortened from $180 \mu\text{s}$ for $X = 0$ to $\sim 10 \mu\text{s}$ for $X = 0.42$ (Fig. 5, curve 1), while the delay of the onset of lasing increased from 220 to $340 \mu\text{s}$ (Fig. 5, curve 2). This effect of nitrogen additions to the laser mixture can be explained by processes of asymmetric VV exchange (see Section 4).

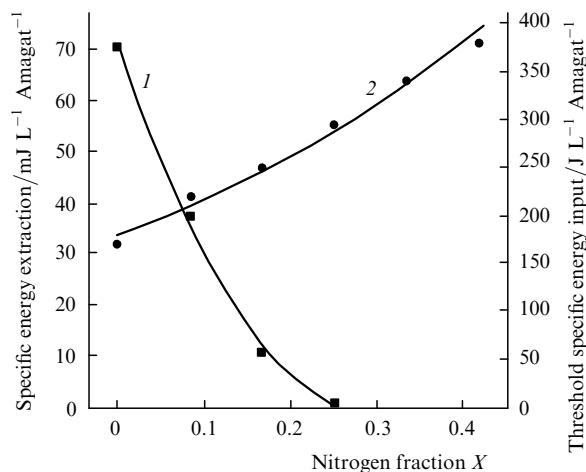


Figure 4. Laser energy extraction at an energy input of $\sim 300 \text{ J} \times \text{L}^{-1} \text{ Amagat}^{-1}$ (1) and threshold specific energy input (2) for the $38 \rightarrow 36$ $P(12)$ transition as functions of the nitrogen fraction X in the CO : He : N₂ = 1 : 4 : X mixture at a mixture density of 0.12 Amagat.

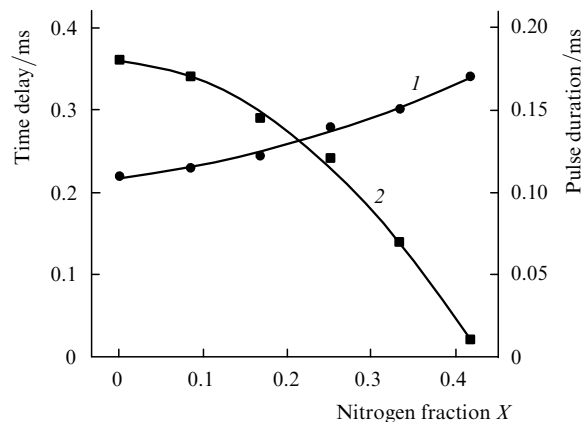


Figure 5. Delay of the onset of lasing (1) and duration of output laser pulse (2) on the $38 \rightarrow 36$ $P(12)$ transition as functions of the nitrogen fraction X in the CO : He : N₂ = 1 : 4 : X mixture at a density of 0.12 Amagat and a specific energy input of $370 \text{ J L}^{-1} \text{ Amagat}^{-1}$.

Replacement of helium with argon, a heavier rare gas, lowers the rate of vibration–translation (VT) relaxation of the upper vibrational levels of the CO molecule in the laser mixture and may therefore lead to a significant increase in the population of these levels. We performed an experimental comparison of the energy characteristics of the overtone CO laser operating on the $37 \rightarrow 35$ $P(13)$ and $38 \rightarrow 36$ $P(14)$ vibration–rotation transitions for two laser mixtures – CO : He = 1 : 6 and CO : Ar = 1 : 6 (Fig. 6). When helium in the laser mixture was replaced with argon, the threshold energy input lowered by 10%–20%, while the maximum laser energy extraction increased by almost

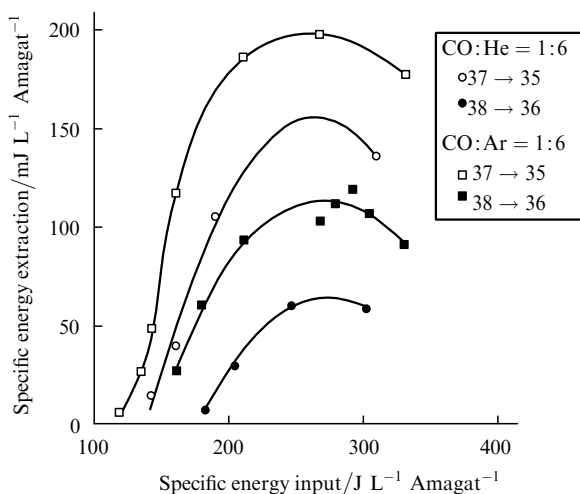


Figure 6. Dependences of the laser energy extraction in the CO : He = 1 : 6 and CO : Ar = 1 : 6 laser mixtures (a density of 0.12 Amagat) on the specific energy input for the 38 \rightarrow 36 $P(14)$ and 37 \rightarrow 35 $P(13)$ transitions.

30 % for the 37 \rightarrow 35 $P(13)$ transition and by nearly a factor of two for the 38 \rightarrow 36 $P(14)$ transition.

4. Theoretical analysis

4.1 Modification of the theoretical model

A comparison of experimental and calculated data performed in Refs [1, 2] displayed a reasonable agreement between them as regards the spectral and energy characteristics of the overtone CO laser. The situation with temporal characteristics is different. The analysis showed that the pulse duration of the overtone radiation and its delay relative to the pump pulse exceed the calculated values. The results of this analysis are consistent with the conclusion of Ref. [9], in which the calculated population dynamics of individual high vibrational levels was compared with experimental data on the optical pumping of the CO molecules, and the conclusion that the evolution of vibrational distribution function in experiment is slower than in theory.

The detailed experimental data on the SSG dynamics on high overtone transitions of the CO molecule, which were presented in the previous Section, allowed us to carry out a detailed comparison between calculated and experimental data. In this case, several improvements were made in the kinetic model to take into account the latest theoretical and experimental data. We adopted the multiquantum vibrational exchange (MVE) model as the physically most substantiated one from the viewpoint of analysis of kinetic processes at high vibrational levels [2, 10, 11].

The rate constants previously employed in this model were corrected in accordance with the results of a recent theoretical paper [12], where the rate constants of several VV-exchange processes between the CO molecules were calculated with the use of a refined quasiclassical technique. Because this set of rate constants is not complete enough, the total array of rate constants was obtained on the basis of data interpolation and extrapolation using the same technique as in Refs [10, 11].

Asymmetric CO($V+2$) + CO(0) \rightarrow CO(V) + CO(1) VV-exchange processes were included in the kinetic model of the CO laser, which became possible with the appearance of Ref. [12]. Furthermore, the asymmetric CO($V+2$) + N₂(0) \rightarrow CO(V) + N₂(1) VV-exchange reactions between vibrationally excited CO molecules and unexcited nitrogen molecules were also included in the model. The rate constants for these reactions in the $T = 100 - 500$ K temperature range were recently derived by quasiclassical calculations in Ref. [13]. Since the resonance in asymmetric exchange with N₂ molecules occurs for $V \approx 38$ and with CO molecules for $V \approx 40$, the exchange with N₂ molecules plays a more significant part. An analysis of the kinetic rate constants for asymmetric VV exchange reactions showed that these processes compete with those of VT relaxation in the depopulation of high vibrational levels of the CO molecule.

In accordance with experimental and theoretical data [14–16], the rate constants of VT relaxation of vibrationally excited CO molecules in collisions with helium atoms were substantially changed. The experimental data of Refs [15, 16] suggest that the rate constants K_{1-0}^{VT} for the CO($V=1$) + He \rightarrow CO($V=0$) + He reactions are significantly lower than the values given in Ref. [17], particularly at low gas temperatures $T < 200$ K, at which the values of rate constants differ several-fold. In Ref. [14], the dependence of VT relaxation rate constants on the vibrational quantum number was determined using quasiclassical calculations. At high vibrational levels, this dependence turns out to be smoother than the dependence that follows from the modified Schwartz–Slawsky–Herzfeld theory [18] previously used in the kinetic model. In the modified model, the calculated data of Ref. [14] were normalised in such a way that the values of K_{1-0}^{VT} rate constants coincided with the data of experimental papers [15, 16].

The spontaneous emission probabilities for transitions at the fundamental frequency and the first and second vibrational overtones of the CO molecule were also updated in accordance with the new data given in Ref. [19].

5. Results of theoretical calculations and comparison with experimental data

The modified MVE model was applied to simulate the SSG dynamics in the CO : He = 1 : 4 laser mixture under the conditions typical of the experiments outlined above: an initial gas temperature of 105 K, a mixture density of 0.18 Amagat, and a specific energy input of 320 J L⁻¹ Amagat⁻¹. We took into account the density variation in the thermal gas expansion caused by its heating due to discharge and also due to VV exchange and VT relaxation (earlier the model of Ref. [20] employed a constant density approximation for the active medium).

The estimates show that the gas density can be assumed constant for several tens of microseconds after the onset of pumping. Then, the expansion proceeds at constant pressure through the egress of the heated active medium to a large buffer volume (~ 0.1 m³). The density variation of the active medium in this case is approximately taken into account within the framework of the uniform model, because the laser beam aperture (20 mm in diameter) in experiments amounted to only a small fraction of the lateral section of the discharge gap (90 \times 160 mm). The density variation of the active medium affects the formation of

vibrational distribution function in VV exchange reactions and hence the SSG dynamics.

We described the time dependence of the active-medium density $N(t)$ by the expression

$$N(t) = N_0 \exp\left(-\frac{t}{\tau}\right) + N_0 \frac{T_0}{T} \left[1 - \exp\left(-\frac{t}{\tau}\right)\right],$$

which simulates a transition to the isobaric regime. Here, N_0 and T_0 are the initial density and temperature of the active medium; $\tau = \Delta r v_s$; Δr is the characteristic transverse dimension of the active medium; and v_s is the sound velocity. A similar approach was earlier employed in Ref. [21]. The translational temperature of the active medium in this case was calculated from the equation

$$\frac{dT}{dt} = \frac{W}{NC_V} + \frac{kT}{NC_V} \frac{dN}{dT},$$

where W is the power density of heat release due to direct heating and vibrational relaxation; C_V is the heat capacity of the active medium; and k is the Boltzmann constant. The density variation of the active medium was accordingly taken into account in the solution of kinetic equations for vibrational level populations as well.

The results of calculations for the four vibrational transitions $26 \rightarrow 24$, $29 \rightarrow 27$, $33 \rightarrow 31$, and $36 \rightarrow 34$ [the $P(12)$ vibration-rotation transition] are given in Fig. 7. A characteristic feature of the calculated dependences is that the gain on the overtone transitions is retained for a relatively long time ($\sim 10^{-3}$ s) after the end of the pump pulse. Fig. 8 serves to compare the $29 \rightarrow 27$ transition data calculated employing the model of Refs [10, 11] and the modified MVE model (curves 1 and 2, respectively). The data derived with the aid of the modified MVE model are characterised by a longer delay time τ_d , a smaller amplitude of the gain, and its slower decay.

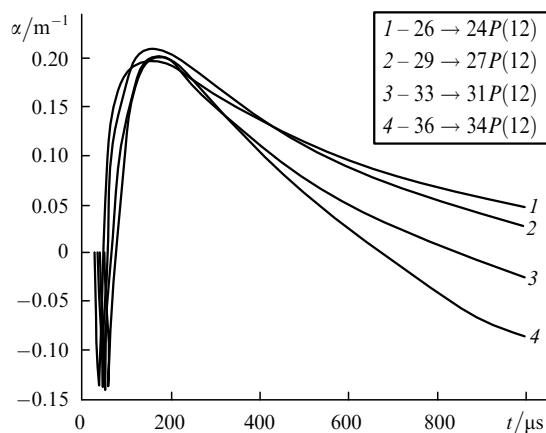


Figure 7. SSG dynamics for the $P(12)$ transition in the $26 \rightarrow 24$, $29 \rightarrow 27$, $33 \rightarrow 31$, and $36 \rightarrow 34$ vibrational bands calculated for the $\text{CO} : \text{He} = 1 : 4$ mixture at a density of 0.18 Amagat and an energy input of $320 \text{ J L}^{-1} \text{ Amagat}^{-1}$.

Fig. 8 also shows the data calculated neglecting asymmetric $\text{CO}(V+2) + \text{CO}(0) \rightarrow \text{CO}(V) + \text{CO}(1)$ processes (curve 3). The asymmetric VV exchange is responsible for a significant increase of the maximum value of gain,

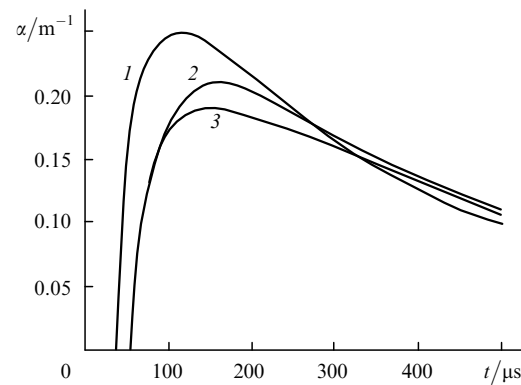


Figure 8. SSG dynamics for the $29 \rightarrow 27 P(12)$ transition calculated using different kinetic models – the model of Ref. [11] (1), the modified model (2), and the modified model neglecting the asymmetric VV exchange between carbon monoxide molecules (3); a $\text{CO} : \text{He} = 1 : 4$ mixture, a density of 0.18 Amagat, and an energy input of $320 \text{ J} \times \text{L}^{-1} \text{ Amagat}^{-1}$.

which is in qualitative agreement with the results of the earlier study of asymmetric VV exchange [22]. It should be emphasised that the effect exerted by asymmetric VV exchange on the results of calculations depends substantially on the choice of VT relaxation rate constants, because these two processes compete at high vibrational levels.

The gain dynamics was calculated employing both the model of Refs [10, 11] and the modified MVE model. Fig. 9 gives a comparison of the calculated and experimental data for the $26 \rightarrow 24$, $29 \rightarrow 27$, $33 \rightarrow 31$, and $36 \rightarrow 34$ transitions. The modified MVE model provides a substantially better description of the experimental data, despite the fact that the time delays τ_d observed in the experiments still exceed the calculated ones. The reason may lie with gas dynamic perturbations, which are responsible for transient optical losses in the laser medium at times of the order of 100 μs that are hard to take into consideration.

Fig. 10a illustrates how the overtone frequency-selective CO-laser efficiency normalised to the peak value depends on the nitrogen concentration in the $\text{CO} : \text{He} : \text{N}_2 = 1 : 4 : X$ mixture for transitions from $32 \rightarrow 30$ to $38 \rightarrow 36$. When the nitrogen concentration is increased from zero to 8.5 %, the efficiency of lasing increases for all vibrational transitions located below the $37 \rightarrow 35$ transition, but lasing vanishes at the $38 \rightarrow 36$ transition. Fig. 10b gives a comparison of the calculated and experimentally measured efficiencies of the overtone CO laser for the $36 \rightarrow 34$, $37 \rightarrow 35$, and $38 \rightarrow 36$ transitions in relation to the nitrogen density in the $\text{CO} : \text{He} : \text{N}_2 = 1 : 4 : X$ laser mixture.

The experimental and theoretical dependences agree quite satisfactorily when the nitrogen concentration is increased, the lasing efficiency increases for the $36 \rightarrow 34$ transition, decreases for the $38 \rightarrow 36$ one, and remains nearly invariable on the $37 \rightarrow 35$ transition. The reason is that a substantial fraction of the flux of vibrational quanta to the upper CO levels is intercepted in the asymmetric VV exchange and is transferred to the lower vibrational levels of the N_2 molecules to be subsequently returned to the CO molecules. Therefore, the asymmetric VV exchange between the CO and N_2 molecules in nitrogen-containing mixtures plays a significant part and should be taken into account in the simulation of the CO-laser active medium.

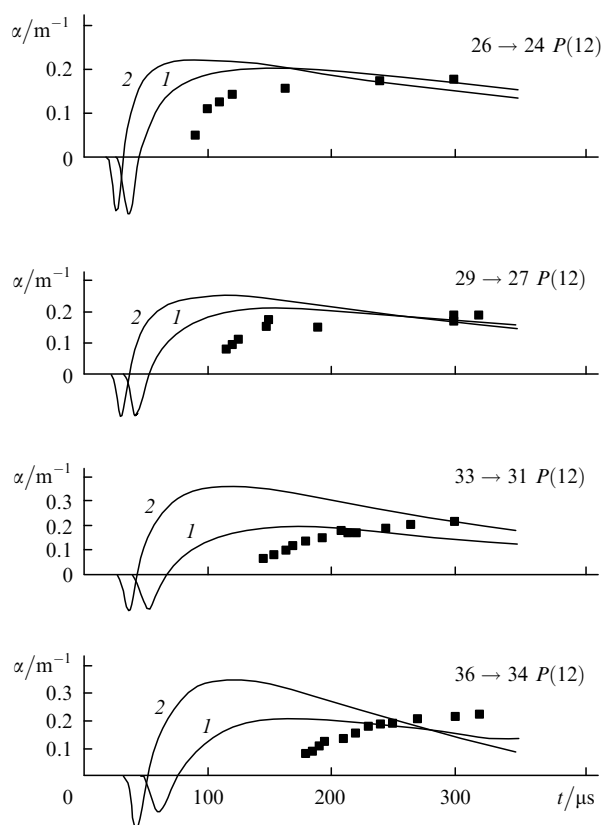


Figure 9. SSG dynamics for the $P(12)$ transition in the $26 \rightarrow 24$, $29 \rightarrow 27$, $33 \rightarrow 31$, and $36 \rightarrow 34$ vibrational bands; (1) modified multi-quantum VV exchange model, (2) kinetic model of Ref. [11]; a CO : He = 1 : 4 mixture, a density of 0.18 Amagat, and an energy input of $320 \text{ J l}^{-1} \text{ Amagat}^{-1}$; the points represent experimental data and the curve represent calculations (the experimental error corresponds to the dimensions of experimental points).

6. Conclusions

We have presented the results of our experimental study of the SSG dynamics for high overtone vibration–rotation transitions of the CO molecule. The gain α_{max} achieved its maximum equal to $\sim 0.4 \text{ m}^{-1}$ for the $33 \rightarrow 31$ $P(12)$ transition in the CO : N_2 = 1 : 9 laser mixture. In the nitrogen-free CO : He = 1 : 4 laser mixture, it was nearly two times lower and almost independent of the vibrational level number. The results of the investigation of the effect of nitrogen on the SSG and the lasing characteristics of the CO laser operating on the $38 \rightarrow 36$ vibrational transition testify that the interaction of N_2 molecules with highly excited CO molecules plays a significant part in the production of population inversion on high vibrational levels. Employing the CO–Ar laser mixture (instead of CO–He) resulted in a significant improvement of the energy characteristics of the laser operating on the extremely high vibrational transitions $37 \rightarrow 35$ and $38 \rightarrow 36$.

The kinetic processes were theoretically analysed using a numerical model. The model was significantly improved in accordance with the recently published data on the rate constants for single- and multi-quantum VV exchange, VT relaxation, and on radiative transition probabilities. Calculations performed for the CO–He mixture showed that the

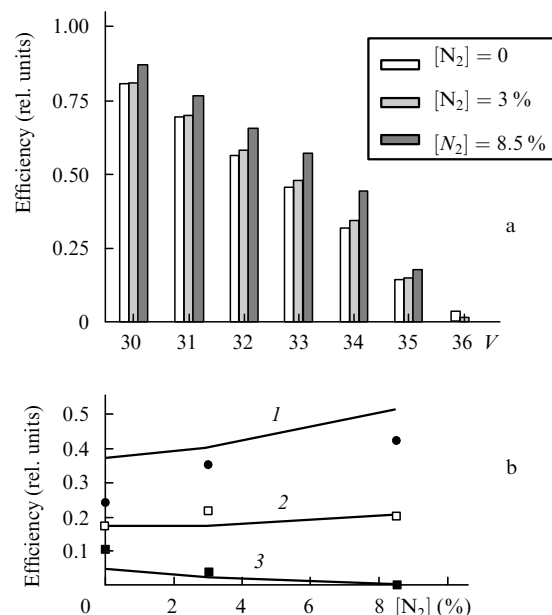


Figure 10. Dependences of the calculated efficiency of the frequency-selective CO laser on the vibrational level V (the $V+2$ transition) for different nitrogen concentrations (a) and on the nitrogen concentration in comparison with the experimental data for the $P(12)$ transition in the $36 \rightarrow 34$ (\bullet , 1), $37 \rightarrow 35$ (\square , 2), and $38 \rightarrow 36$ (\blacksquare , 3) vibrational bands. A CO : He = 1 : 4 mixture, a density of 0.18 Amagat, and an energy input of $320 \text{ J l}^{-1} \text{ Amagat}^{-1}$.

gain on the first-overtone vibrational transitions is retained for a relatively long time ($\sim 1 \text{ ms}$) after the pump pulse and the maximum gain on high transitions amounts to approximately 0.2 m^{-1} for a nitrogen-free mixture. These data agree well with experimental data, but the experimentally observed time delays τ_d were found to exceed the calculated ones. One reason for the discrepancy between the theory and experiment may lie in discharge-initiated gas dynamic perturbations, which introduce additional radiation losses for time periods of the order of $100 \mu\text{s}$.

The theoretical analysis of the effect of small additions of nitrogen to the CO–He active medium was performed on the basis of a modified kinetic model. As in experiments, increasing the nitrogen concentration in the laser mixture resulted in an increase of the calculated efficiency of lasing of the CO laser on vibrational transitions located below the $37 \rightarrow 35$ transition and in the disappearance of lasing on the $38 \rightarrow 36$ transition. This is caused by the asymmetric VV exchange between nitrogen molecules and highly excited carbon monoxide molecules: $\text{CO}(V+2) + \text{N}_2(0) \rightarrow \text{CO}(V) + \text{N}_2(1)$. Our investigation demonstrated that these processes should be taken into account in the analysis of the dynamics of the population distribution function at high vibrational levels of the CO molecule.

Acknowledgements. The authors thank H. Ackermann, J. McIver, and M. Stickley for their help in management of this work, and also N.G. Turkin, Yu.V. Terekhov, S.V. Vetoshkin, and A.Yu. Kozlov for their assistance in experiments.

This work was supported by the Russian Foundation for Basic Research (Grant No. 99-02-17553), the ‘Integration’ Federal Dedicated Programme (Project No. AO155), the

International Science and Technology Centre, and the European Office for Research and Development (Grant No. 1865-P).

References

1. Basov N.G., Ionin A.A., Kotkov A.A., et al. *Kvantovaya Elektron.*, **30**, 771 (2000) [*Quantum Electron.*, **30**, 771 (2000)].
2. Basov N.G., Ionin A.A., Kotkov A.A., et al. *Kvantovaya Elektron.*, **30**, 859 (2000) [*Quantum Electron.*, **30**, 859 (2000)].
3. Buzykin O.G., Ionin A.A., Ivanov S.V., et al. *Laser and Particle Beams*, **18**, 697 (2000).
4. Buzykin O.G., Ivanov S.V., Ionin A.A., et al. *Opt. Atmos. Okeana*, **14**, 400 (2001).
5. Buzykin O.G., Ivanov S.V., Ionin A.A., et al., in *VIIth International Conference 'Laser and Laser-Information Technologies: Basic Problems and Applications'* (Shatura–Vladimir State University, Vladimir: IPLIT RAN, 2001) p. 75.
6. Ionin A.A., Klimachev Yu.M., Kotkov A.A., et al., in *Proc. Int. Conf. LASERS 2000* (STS Press, McLean, VA, USA, 2001) p. 309.
7. Vetoshkin S.V., Ionin A.A., Klimachev Yu.M., et al., in *Proceedings of the Scientific Session of the Moscow Institute of Engineering Physics (MIFI)-2001* (Moscow: MIFI Publ., 2001) Vol. 4, p. 45.
8. Urban W. *Laser und Optoelektronik*, **23**, 56 (1991).
9. Porshnev P.I., Wallaart H.L., et al. *Chem. Phys.*, **213**, 111 (1996).
10. Ionin A.A., Klimachev Yu.M., Konev Yu.B., et al. *Kvantovaya Elektron.*, **30**, 573 (2000) [*Quantum Electron.*, **30**, 573 (2000)].
11. Ionin A.A., Klimachev Yu.M., Kotkov A.A., et al. *J. Phys.D: Appl. Phys.*, **34**, 2230 (2001).
12. Coletti C., Billing G.D. *J. Chem. Phys.*, **113**, 4869 (2000).
13. Cacciatore M., Kurnosov A., Napartovich A., in *Proc. Int. Conf. ICPEAC 2001* (Santa Fe, New Mexico, USA, 2001).
14. Cacciatore M., Capitelli M., Billing G.D. *Chem. Phys.*, **82**, 1 (1983).
15. Reid J.P., Simpson C.J.S.M., et al. *J. Chem. Phys.*, **103**, 2528 (1995).
16. Reid J.P., Simpson C.J.S.M. *J. Chem. Phys.*, **107**, 9929 (1997).
17. Allen D.C., Price T.J., Simpson C.J.S.M. *Chem. Phys.*, **41**, 449 (1979).
18. Smith N.S., Hassan H.A. *AIAA J.*, **14**, 374 (1976).
19. Langhoff S.R., Bauschlicher C.W. *J. Chem. Phys.*, **102**, 5220 (1995).
20. Ionin A.A., Klimachev Yu.M., Kotkov A., et al. Preprint No.11 (Moscow: P.N. Lebedev Physics Institute, Russian Academy of Sciences, 1998).
21. Akishev Yu. S., Dem'yanov A.V., Kochetov I.V., et al. *Teplofiz. Vys. Temp.*, **20**, 818 (1982).
22. Dem'yanov A.V., Kochetov I.V., Napartovich A.P., et al. *Teplofiz. Vys. Temp.*, **18**, 916 (1980).